NASA

Technical Memorandum 80288

Magnetic Field Studies at Jupiter By Voyager I: Preliminary Results

N. F. Ness, M. H. Acuna, R. P. Lepping,
L. F. Burlaga, K. W. Behannon, F. M. Neubauer

APRIL 1979

National Aeronautics and
Space Administration

Goddard Space Flight Center
Greenbelt, Maryland 20771

MAGNETIC FIELD STUDIES AT JUPITER BY VOYAGER 1: PRELIMINARY RESULTS

Norman F. Ness

Mario H. Acuna

Ronald P. Lepping

Leonard F. Burlaga

Kenneth W. Behannon

Goddard Space Flight Center

Greenbelt, MD 20771

and

Fritz M. Neubauer

Technische Universität

Braunschweig, FRG

Submitted to Science: 3 April 1979

Revised: 11 April 1979

ABSTRACT

This paper will discuss highlights of results obtained by the Goddard Space Flight Center magnetometers on Voyager 1 concerning the large scale configuration of the Jovian bow shock and magnetopause, and the magnetic field in both the inner and outer magnetosphere. We find there is evidence that a magnetic tail extending away from the planet on the night-side is formed by the solar wind-Jovian field interaction. This is much like Earth's magnetosphere but is a new configuration for Jupiter's magnetosphere not previously considered from earlier Pioneer data. We report on the analysis and interpretation of magnetic field perturbations associated with intense electrical currents (approximately 5×10^6 amps) flowing near or in the magnetic flux tube linking Jupiter with the satellite Io and induced by the relative motion between Io and the co-rotating Jovian magnetosphere. These currents may be an important source of heating the ionosphere and interior of Io through Joule dissipation.

INTRODUCTION

The Voyager magnetic field experiment consists of dual low field (LFM) and high field (HFM) triaxial fluxgate magnetometer sensors and associated electronics with extensive redundancy for high reliability as well as correction for the spacecraft's magnetic field (1). One LFM is located at the tip of a 13 m. boom while the other is mounted 5.6 m. inboard. Total weight of sensors plus electronics including the 2 HFM instruments is 5.6 kilograms and the power required is 2.2 watts. During encounter, the LFMs automatically ranged through 7 (of 8 possible) scales for maximum sensitivity ($\pm$8.8 nanotesla (nT) to $\pm$6400 nT, with quantization steps of 0.0044 nT to 3.12 nT). The sensor equivalent RMS noise is 0.006 nT (0.01-8.3 Hz). The dual magnetometer method and the estimation of zero offsets yield a preliminary accuracy of $\pm$0.2 nT $\pm$0.1% of full scale. The vector field was measured every 60 milliseconds, and averages over 1.92 sec, 48 sec, and 16 min. are used in this paper.

The present results are based upon preliminary experiment data records (EDRs), some of which are incomplete, and predicted supplementary EDRs which describe the predicted trajectory and orientation of the spacecraft. Voyager 1 executed several maneuvers during the encounter period which are not yet accurately described, and these data have been omitted in our analyses. The experiment operated flawlessly throughout the encounter, and no deleterious effects of the intense radiation environment and exposure has been noted in the data processed to date.

BOW SHOCK, MAGNETOPAUSE AND MAGNETOSPHERE

Voyager 1 crossed the bow shock of Jupiter for the first time at 1434 UT on 28 February (Day 59) 1979 at a Jovicentric distance of 85.7 R_J (R_J = radius of Jupiter). There were a total of five bow shock encounters inbound to periapsis as shown in Figure 1, the final one on Day 61 at 1308 UT. Also shown are magnetopause crossings, the first and last of which occurred at 1956 UT, Day 60, and 0220 UT, Day 62, respectively. Nine crossings were tentatively identified from the magnetic field data, with other less certain possibilities remaining.

Magnetic coplanarity was used to estimate the direction perpendicular to the bow shock surface . This yielded an average for the set of five: $\langle\delta\rangle = -4^\circ \pm 13^\circ$ and $\langle\lambda\rangle = 171^\circ \pm 9^\circ$, where δ and λ are solar equatorial plane referenced latitude and longitude, respectively ($\lambda \equiv 180^\circ$ is sunward). The nine magnetopause candidates were analyzed by determining the plane of minimum variance (2) of the magnetic field variation applied to 1.92s averages. An average of $\langle\delta\rangle = 3^\circ \pm 13^\circ$ and $\langle\lambda\rangle = 165^\circ \pm 11^\circ$ was obtained with a straight line segment representing $\langle\lambda\rangle = 165^\circ$ shown in Figure 1. The "thickness" of the magnetopause transition zones ranged from 3 to 13 min., averaging 6.5 min.

Identifications of the outbound magnetopause and bow shock crossings are not complete at this date (3/29/79), but Figure 1 shows first and last magnetopause candidates (MP-A&B), at 0033 UT on Day 74 and at 0520 on Day 75, respectively, and for the first and last bow shocks (BS-A&B) at 0706 UT on Day 77 and 1305 on Day 81, respectively. The minimum variance analysis, as applied to MP-A data, yielded $\delta = 21^\circ$ and $\lambda = 127^\circ$. No other outbound magnetopause or bow shock

crossing has been analyzed. Note that more precise bow shock normals will be determined when plasma data are available.

A model was constructed of a nominal magnetopause surface represented by a hyperbola in the Jupiter orbital plane assuming symmetry about the x-axis (see Figure 1). The curve was constrained to intersect the inbound and outbound midpoints (i.e., points midway between first and last crossings), and the slope inbound was made to agree with a $\lambda = 165^{\circ}$ surface normal. Outbound the model predicts $\lambda = 126^{\circ}$, which agrees very well with $\lambda = 127^{\circ}$ observed. Similarly a hyperbolic fit was made to the bow shock crossings, adjusting the position of the focus and the y-axis scale factor to force bow shock midpoint intersections. The average of the inbound bow shock normals was believed to be too uncertain to contribute good slope information. The predicted value of λ for the normal of the midpoint inbound bow shock set is $\lambda = 165^{\circ}$, which agrees well with $\lambda = 171^{\circ}$ given above. The model magnetopause and bow shock distances at the subsolar point give a ratio of 57/72 = 0.79, compared to Earth's which is typically 0.69. The observed magnetopause crossings do not occur in the system III (1965) longitude interval predicted from Pioneer 10 and 11 data (3).

Figure 2 presents a summary of the magnetic field encounter data set, showing magnitude and mean component fluctuations (RMS) observed during 16 min. averaging periods. A prominant feature is the recurrent decrease in the magnetic field intensity at approximately 5 or 10 hour intervals and always associated with increases in the RMS. The steady increase of the RMS near periapsis is due to spatial gradients of the magnetic field in the inner magnetosphere and not

to intrinsic temporal fluctuations as seen elsewhere. The first peak in the RMS after closest approach (CA) at $\approx$ 1500 UT is in part due to the Io flux tube currents. The dips in the field intensity correspond to passage of the spacecraft through a near equatorial current sheet, and usually occur in close proximity to the extended magnetic equatorial plane. In the inner magnetosphere, i.e., at distances <12 R_J, the magnitude of the observed field was consistently below that predicted from the model field O_4 (4) by several hundred gammas. This suggests large scale azimuthal currents in the Jovian magnetosphere.

The traditional method for the analysis and representation of planetary magnetic field data utilizes orthogonal spherical harmonic functions and assumes the magnetic field is derivable from a scalar potential. This is equivalent to assuming that there is no current flowing in the region of observations from which the unknown coefficients for the expansion are derived. Formal analyses of data taken within the inner magnetosphere of Jupiter are summarized in Table I. The tilt and longitude of the dipole term are seen to be very close to the O_4 values. However, the magnitude of the moment obtained by these analyses is approximately 5% less than the O_4 values. We do not believe this represents a secular change of the planetary field but interpret it to be primarily due to the failure of the scalar potential mathematical representation to be physically valid in the regions of space in which the observations were conducted. Future studies will address this issue.

MAGNETODISC AND MAGNETOTAIL CURRENT SHEETS

Between 6 and 16 March (Days 65-74) measurements were performed in the night-side Jovian magnetosphere (see Figures 1 & 2). During this period, intervals of perturbed field were observed during which $|\underset{\sim}{B}|$ was reduced by $\geq 80\%$, the field had a southward component, and, through Day 68, its azimuth (λ) changed. The character of these depressed field events is consistent with a diamagnetic plasma sheet and a thin embedded current sheet in which the direction of $\underset{\sim}{B}$ changed.

Decreased fields in the plasma sheet were periodically observed out to the vicinity of the magnetopause, but the current sheet was not crossed beyond a distance of 80 R_J. During each 10-hr period out to 80 R_J, the spacecraft spent on average 3.2 ± 0.8 hours south of the current sheet and 6.8 ± 0.7 hours above it (the uncertainties are one σ values). Beyond 80 R_J, the depressions in $|\underset{\sim}{B}|$ were seen at intervals of 10.0 ± 0.9 hours. Outside of the plasma sheet the observed field was extremely steady and oriented almost parallel to the heliographic equatorial plane ($\delta \sim 0^\circ$) at an angle of $\lambda \sim 35^\circ$ when the spacecraft was north of the current sheet and $\sim 215^\circ$ when south. These angles are consistent with the magnetic field approaching the direction parallel to the magnetopause at large distances (see Figure 1, MP-A&B), as well as with the earlier Pioneer 10 interpretation of a spiralling of the field (5,6,7,8).

Figure 3 shows the spacecraft locations during the perturbed field intervals in terms of both the longitude and radial distance. The south-to-north and north-to-south current sheet crossings are seen as the lower and upper sets, respectively. Both types

of crossings were delayed in longitude (and time) relative to the prediction (5) for a rigid disc (dashed lines). The magnitude of the delay increases with distance from the planet. It is significant that the delay and its change with distance were more pronounced for the north-to-south crossings than for the south-to-north cases. That Voyager did not cross the current sheet beyond 80 R_J implies a warping of the sheet such that it did not reach the latitude of the spacecraft.

Several types of distortion of an equatorial disc-shaped current sheet can give an increasing delay (5,6). On the basis of the Pioneer 10 observations (7) a spiral-shaped distortion has been considered by several investigators (8). Such a distortion implies a straight line on a system III (1965) longitude-R_J plot of the current sheet crossings. Figure 3 shows such lines drawn with the slope found (8) from a fit to the Pioneer 10 outbound current sheet crossings. The south-to-north Voyager 1 crossings are closer to the curve for an undistorted disc, whereas the north-to-south crossings are closer to the curve for a disc with spiral distortion. A distortion due to centrifugal forces also has been suggested (7), but this implies symmetry between the two types of crossings.

Another possible type of current sheet distortion, not considered in the literature for Jupiter, is a bending of the tailward part of the equatorial current sheet toward being parallel to the solar wind flow direction as an extended magnetotail like Earth's forms. For a spacecraft located above the Jovian equatorial plane, this distortion would appear maximum when the line of intersection between the magnetic equatorial plane and the Jovian equatorial plane has a dawn-dusk orientation and the northern half of the current disc is tailward.

Voyager south-to-north crossings occurred near times when the sheet deformation was small and therefore were more consistent with the rigid disc model. The north-to-south crossings occurred when the bending of the tailward half of the current sheet away from the magnetic equatorial plane was large, and thus they occurred with a lag, relative to magnetic equatorial plane crossings, that increased with distance.

Further support for the concept of a transition to a magnetic tail configuration with increasing distance comes from examination of the structure of the observed current sheets. One can distinguish two classes of current sheets. One is characterized by a decrease in magnetic field intensity to a minimum significantly different from zero ($\geq$ several gammas) and a rotation of field direction by $<180^{\circ}$, and the other by a decrease in magnetic field intensity to nearly zero ($\lesssim 1\gamma$) and an $\approx 180^{\circ}$ change (reversal) in magnetic field direction. Examples of the first class of current sheets are shown in the top panel of Figure 4. A minimum variance analysis showed that the magnetic field direction in crossings A and C changed by means of a rotation of one component of $\underset{\sim}{B}$ in a plane whose normal was $\delta = -75^{\circ}$ in case A and $\delta = -86^{\circ}$ in case C. Current sheets of this class were observed principally inbound and near Jupiter outbound.

Examples of the second class of current sheets are shown at the bottom of Figure 4. They resemble the changes that are expected for a magnetic "tail", and indeed they were observed when Voyager 1 was tailward of and at larger distances from Jupiter. The difference between the two classes of crossings shown in Figure 4 may thus represent a transition from corotating closed field lines near Jupiter ($\lesssim 25\ R_J$) to more distended or open field lines farther from the planet as the magnetic tail region was penetrated by Voyager 1.

IO FLUX TUBE OBSERVATIONS

A distinct magnetic field perturbation due to intense electrical currents induced by Io was observed when the spacecraft approached the minimum distance of 20500 km south of the satellite at 1505 UT March 5. Passage through Io's flux-tube, the ensemble of Jovian field-lines penetrating the satellite, had been predicted to occur between 1502 and 1507 UT based on the GSFC O_4 model. No noticeable change in field intensity was detected but there were significant directional changes.

To study the perturbation, the components of the local Jovian field were individually estimated by a regression analysis excluding the data most obviously affected by Io's presence. (The present analysis is still preliminary because of the lack of final attitude-orbit information). After subtraction of the Jovian field, the perturbation field vectors, $\Delta\vec{B}$, lie approximately in a plane transverse to the background field. We define a right-handed orthogonal coordinate system centered at, and moving with, Io with the z-axis parallel to the background field and the x-axis located in the plane of the z-axis and the direction of corotational magnetospheric flow at Io. Inspection of the data at the highest possible time resolution shows that the field variation near Io is indeed very smooth and few, if any fluctuations are observed at short time scales. The maximum perturbation is 94 nT at 1505 UT.

Figure 5 shows the components of the measured magnetic perturbation field together with least-mean-squares fits of a line current source antiparallel to the z-axis and a two-dimensional (2D) dipole source

at locations $\vec{x}_D = (x_D, y_D)$ also determined by the best fit. The field of the 2D-dipole source is given by $\Delta\vec{B} = -\mu_o \nabla\Psi$ where

$$\Psi(\vec{x}) = \frac{\vec{m} \cdot (\vec{x} - \vec{x}_D)}{2\pi|\vec{x} - \vec{x}_D|^2} \qquad (1)$$

with the position vector $\vec{x} = (x,y)$ and the 2D-magnetic moment $\vec{m} = (m_x, m_y)$ defined in the x, y-plane. We note that a 2D-dipole occurs as the lowest order term in the expansion of a system of currents parallel or antiparallel to the z-axis with zero net current. $\vec{m}$ can simply be considered as the magnetic moment per unit length in the z-direction. For two opposite line currents its value $|\vec{m}|$ is given by current times distance. Figure 6 shows the trajectory projected on the x, y-plane together with the vectors $\Delta\vec{B}$ and the best-fit 2D-dipole. This analysis shows that the 2D-dipole fit is quite reasonable and is much better than the line current fit. It should be noted that the small linear extent of the magnetic field anomaly, FWHM = 9000 km, when compared to the distance to Io, 20500 km, and the lack of intensity perturbations, effectively rule out an intrinsic field of Io as the source of the observed anomaly.

The smooth variation of $\Delta\vec{B}$ and the good fit to a two dimensional dipole are in agreement with the idea that Voyager passed very close to a current system with upward and downward currents of about equal magnitude along the z-axis but did not actually penetrate the region of maximum current flow. This observational result is in agreement with the physical concept of Io's role as a unipolar generator proposed 10 years ago (9) and later extended (10). The electric field is set up in Io due to its motion relative to the corotating

magnetospheric plasma, and this drives a current system through the conducting path formed by Io, Io's ionosphere, field-aligned currents in the Jovian magnetosphere and transverse currents through the Jovian ionosphere. In a more accurate description the field-aligned currents are replaced by a current system of standing Alfvén waves, which also involve non-field-aligned current components (11). A more refined physical modeling of the observations is deferred to a later study.

The large currents may be the source for offset of the location of the Io flux tube foot-print near Jupiter, which can explain the asymmetry of the observed Io-modulated decametric emission pattern (9,13). Note that the 2D-dipole is offset by 7000 km out of 20500 km or an equivalent angle of 19^{o}. This offset is, of course, the reason for the failure of Voyager 1 to penetrate the flux tube as planned.

The power dissipation implied in the current loop set up by Io's interaction with the Jovian magnetosphere leads to a Joule heating of $P \approx 10^{12}$ watts. This value is rather model independent and is given by $P = m_x \cdot E_{Io}$ where $E_{Io} = v_{rel} \cdot B_{Io}$ with $v_{rel} = 57$ km/s and $B_{Io} \approx 1900$ nT. The value of P is close to the value obtained from tidal dissipation (12). Since electrical currents flow in paths of least resistance, internal hot spots in Io might develop where the the current cross-section narrows in the interior of Io. As the temperature rises, so does the conductivity, and this may lead to an intensification or runaway of energy dissipation in the form of Joule heating. We point to the possible role of this Joule heating for Io and the Io plasma torus.

REFERENCES

(1) K. W. Behannon, M. H. Acuna, L. F. Burlaga, R. P. Lepping, N. F. Ness, F. M. Neubauer, Space Sci. Revs. 21, 235, 1977.

(2) B. U. O. Sonnerup and L. J. Cahill, J. Geophys. Res., 72, 171, 1967.

(3) A. J. Dessler and V. M. Vasyliunas, Geophys. Res. Letters, 6, 37, 1979.

(4) M. H. Acuna and N. F. Ness, J. Geophys. Res., 81, 2917, 1976.

(5) J. A. Gledhill, Nature, 214, 156, 1967; C. K. Goertz, J. Geophys. Res., 81, 3368, 1976.

(6) L. J. Gleeson and W. I. Axford, J. Geophys. Res., 81, 3403, 1976.

(7) E. J. Smith, L. Davis, Jr., D. E. Jones, P. J. Coleman, Jr., D. S. Colburn, P. Dyal, C. P. Sonett, A. M. A. Frandsen, J. Geophys. Res., 79. 3501, 1974.

(8) T. G. Northrop, C. K. Goertz, M. F. Thomsen, J. Geophys. Res., 79, 3579, 1974; D. E. Jones, E. J. Smith, L. Davis, Jr., D. S. Colburn, P. J. Coleman, Jr., P. Dyal, C. P. Sonett, Utah Acad. Sci. Arts Lett. Proc., 51, 153, 1974; A. Eviatar and A. I. Ershkovich, J. Geophys. Res., 81, 4027, 1976; M. G. Kivelson, P. J. Coleman, Jr., L. Froidevaux, R. L. Posenberg, J. Geophys. Res., 83, 4823, 1978.

(9) J. H. Piddington and J. F. Drake, Nature, 217, 935, 1968; P. Goldreich and D. Lynden-Bell, Ap. J., 156, 59, 1969.

(10) S. D. Shawhan, C. K. Goertz, R. F. Hubbard, D. A. Gurnett and G. Joyce, in The Magnetospheres of the Earth and Jupiter (ed. V. Formisano), Reidel, Dordrecht, 1975; J. H. Piddington, The Moon, 17, 373, 1977.

(11) S. D. Drell, H. M. Foley and M. A. Ruderman, J. Geophys. Res., 70, 3131, 1965.

(12) S. Peale, P. Cassen, R. T. Reynolds, Science, 203, 892, 1979.

(13) See for example Fig. 2 R. A. Smith in Jupiter: The Giant Planet ed. by T. Gehrels, pp.1146-1189, U. of AZ, 1976.

(14) We are indebted to our colleagues in the Voyager project for discussions of these early results and the entire Voyager project team for the success of this experiment. We especially appreciate the dedicated support of Glenn Sisk, Dr. Ernest Franzgrote and J. Tupman of JPL. We further acknowledge the contributions of C. Moyer, J. Scheifele, J. Seek and E. Worley to the design, development and testing at GSFC of the experiment instrumentation, and of T. Carlton, P. Harrison, D. Howell, W. Mish, L. Moriarty, A. Silver and M. Silverstein in the GSFC data analysis team to the success of the rapid MAG and PLS data processing system. F. M. Neubauer was supported financially by the German Ministry of Science and Technology (BMFT).

FIGURE CAPTIONS

Figure 1 Voyager 1 Jupiter encounter trajectory in Jupiter-centered orbital coordinates (x-y plane is the orbital plane, +x toward the sun, +z northward). Day of year is labeled on trajectory, which remains within 12.1 R_J of Jupiter's orbital plane over interval shown.

Figure 2 The magnetic field magnitude and pythagorean mean RMS deviation for approximately ±8 days around closest approach (CA) to Jupiter which occurred at 1205 UT on Day 64, 1979. Inbound bow shock (BS) and magnetopause (MP) crossings times are denoted, as are a plot scale change and the Io flux tube RMS peak.

Figure 3 The Jovicentric distance and extent in System III longitude of perturbed field regions. The gap in a bar marks the longitude at which the minimum field magnitude was observed. Out to R~80 R_J, the lower set of bars represent south-to-north transitions and the upper set the north-to-south crossings. Dashed curves indicate the longitudes at which the magnetic equator (rigid rotating disk) was crossed by the spacecraft (see text).

Figure 4 Jovian field intensity dips or decrease events. The top panel illustrates the class seen near Jupiter. The bottom panel illustrates a second class which is observed at large distances outbound. The latter resemble "neutral" sheet crossings seen in the Earth's magnetic tail. The angles are given in heliographic coordinates.

Figure 5 Comparison of observed perturbation magnetic field components ΔB_x, ΔB_y and best fit magnetic fields for twin oppositely directed currents and for a line current. The line current is located at x_D = 5130 km and y_D = -3730 km and has a strength of 1.1×10^6 amps.

(Fig. 5 continued)

The twin currents are located at x_D = 6950 km and y_D = -200 km with a strength 1.3×10^{10} amp·km.

Figure 6 Magnetic perturbation vector $\Delta\vec{B}$ in the x-y plane of coordinates used in our analyses (see text). The dipole source can be represented by a current of 4.8×10^6 amps distributed over a cylindrical surface of one Io diameter with variable intensity according to a cosine law. The uncertainties of the regression analysis may be expressed as follows: $\mu_o |m| / 2\pi d_{min}^2 = 85 \pm 10$ nT, where d_{min} is the distance of the dipole from the trajectory in the x, y-plane and $|\underline{m}|$ the dipole moment. In addition $|\underline{m}| = (1.2 \pm 0.4) \times 10^{10}$ amp·km and $y_D = -700 \pm 700$ km. The direction of the 2D-dipole moment is shown by the large arrow and is seen to be 15^o outward from the direction of Io's velocity.

MODEL	RADIAL EXTENT	NO.	MAGNITUDE	θ	∅	RMS	CN
I1E1	$< 9R_J$	119	3.98±.02	9.6±.2	194°±2°	73	4
I2E1	$< 9R_J$	119	4.09	10.1	189°	30	32
I1E1	$< 6R_J$	69	3.76	10.6	189°	68	13
I2E1	$< 6R_J$	69	3.84±.04	13.3±.3	190°±2°	11	
I3E0	$< 6R_J$		4.28	9.6°	202°	Model O_4	

TABLE I - PRELIMINARY JOVIAN DIPOLE ANALYSES

MODEL IjEk includes spherical harmonic terms up to order j for internal sources and k for external. No. is number of data points at 4.8 minute intervals, magnitude in units Gauss-R_J^3, tilt and System III (1965) longitude in degrees. RMS is pythagorean mean of component RMS values and CN is the precondition number used in the matrix inversion.

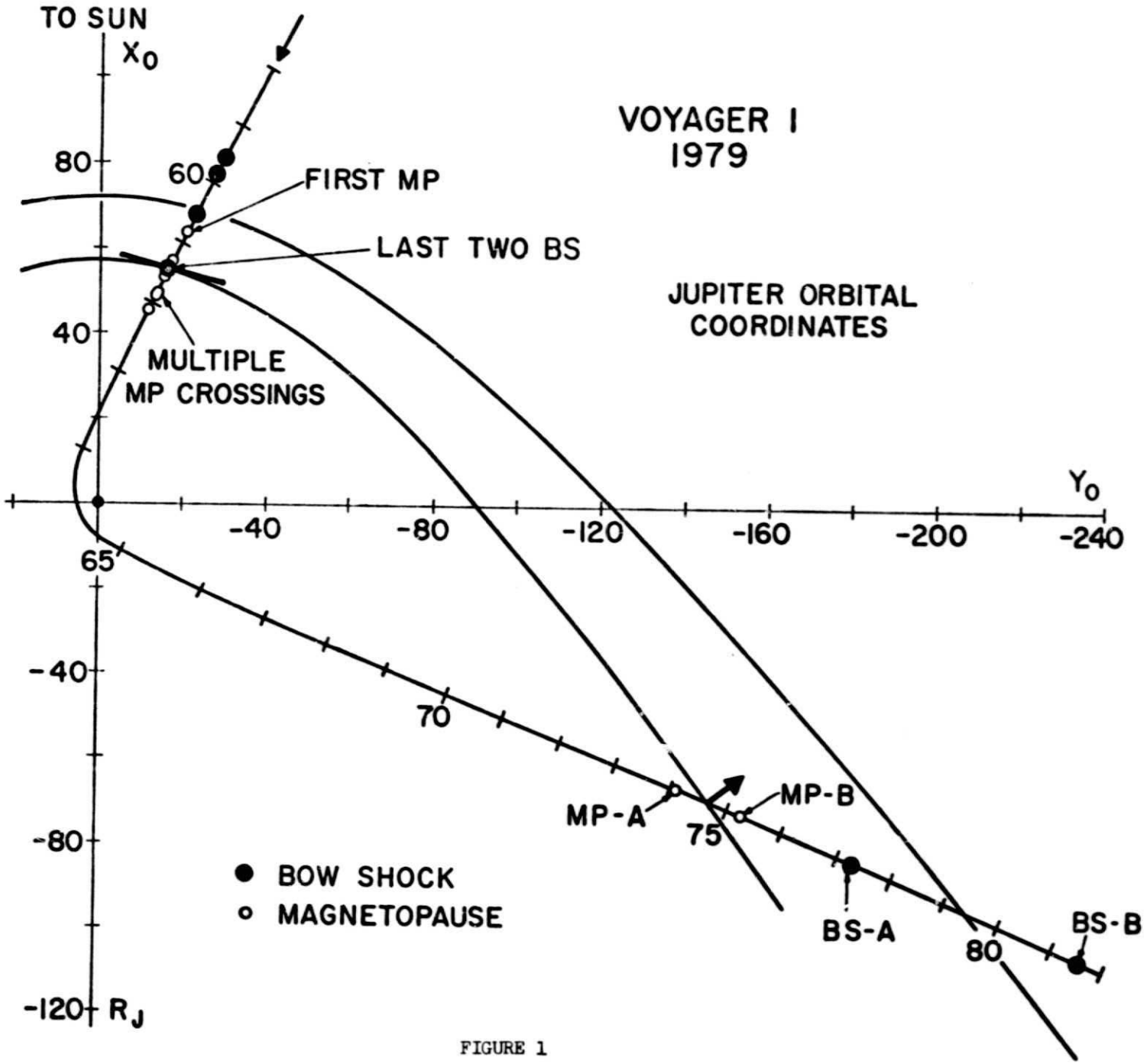
TO SUN
X_O
VOYAGER 1
1979
JUPITER ORBITAL
COORDINATES
FIRST MP
LAST TWO BS
MULTIPLE
MP CROSSINGS
Y_O
80
60
40
-40
-80
-120
-160
-200
-240
65
70
75
80
-40
-80
-120
R_J
MP-A
MP-B
BS-A
BS-B
BOW SHOCK
MAGNETOPAUSE

FIGURE 1

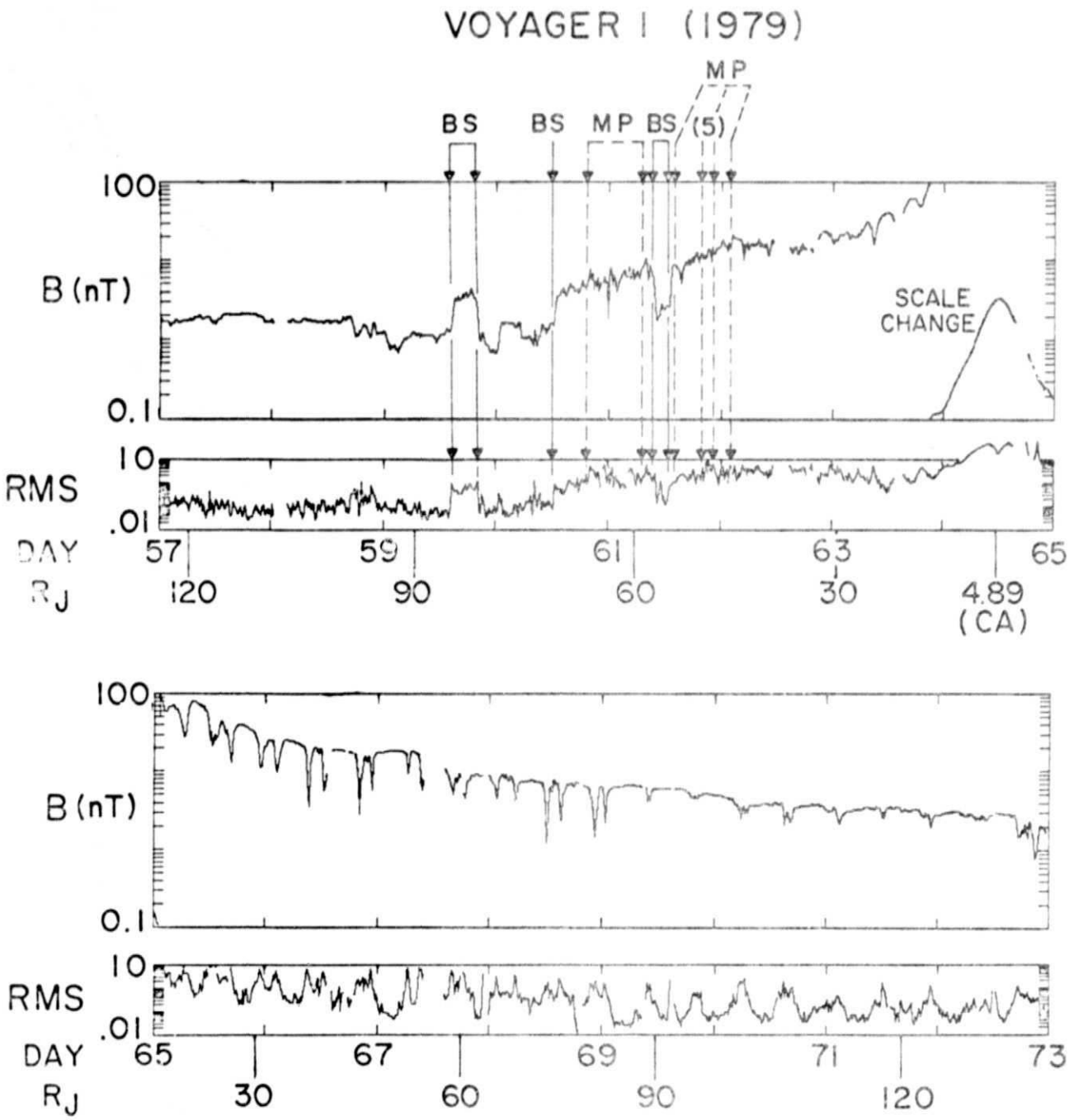
VOYAGER I (1979)
MP
BS
BS
MP
BS
(5)
100
B (nT)
0.1
SCALE
CHANGE
10
RMS
.01
DAY
57
59
61
63
65
R_J
120
90
60
30
4.89
(CA)
100
B (nT)
0.1
10
RMS
.01
DAY
65
67
69
71
73
R_J
30
60
90
120

FIGURE 2

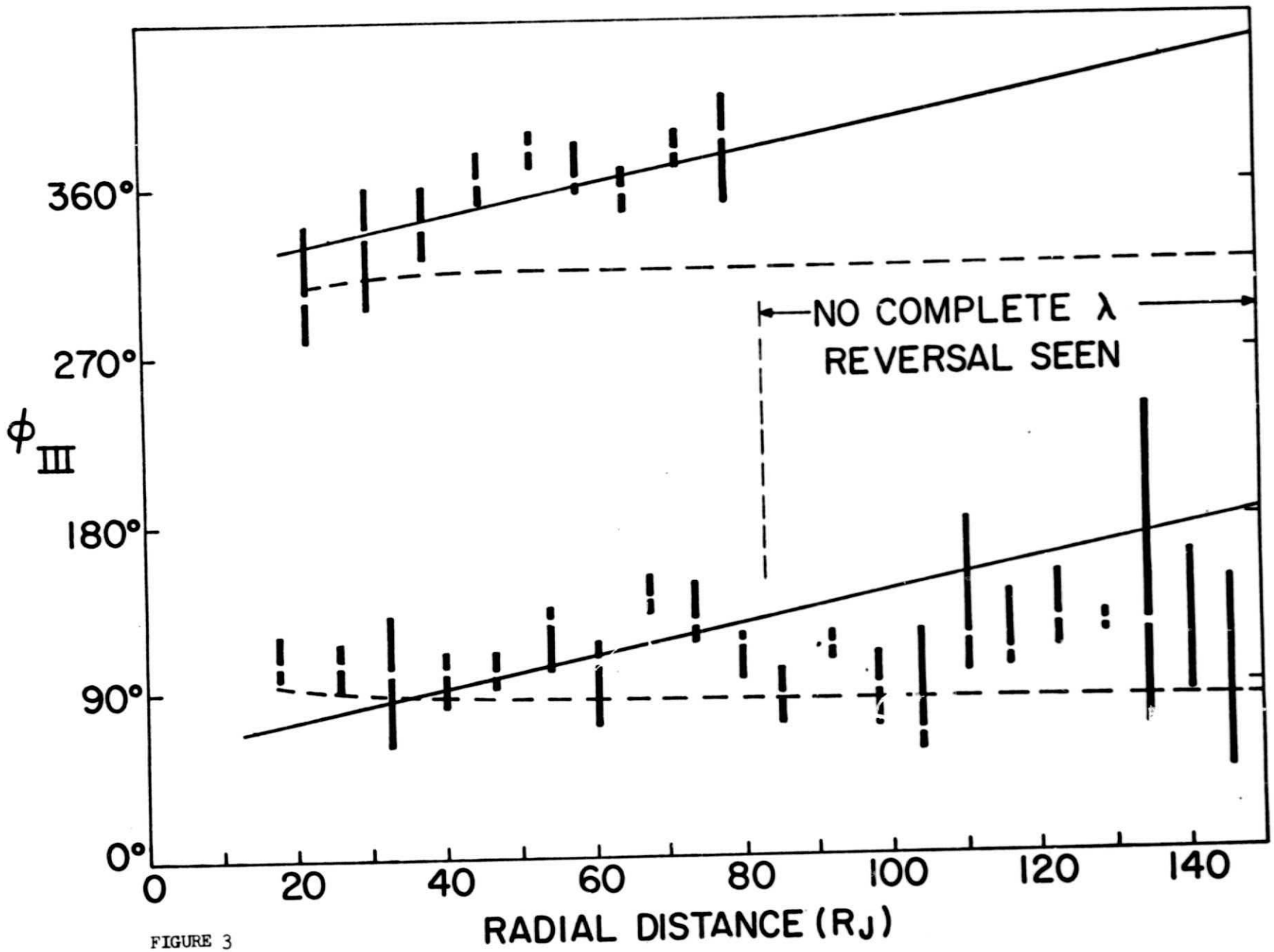
360°
270°
ϕ_{III}
180°
90°
0°
NO COMPLETE λ
REVERSAL SEEN
0
20
40
60
80
100
120
140
RADIAL DISTANCE (RJ)

FIGURE 3

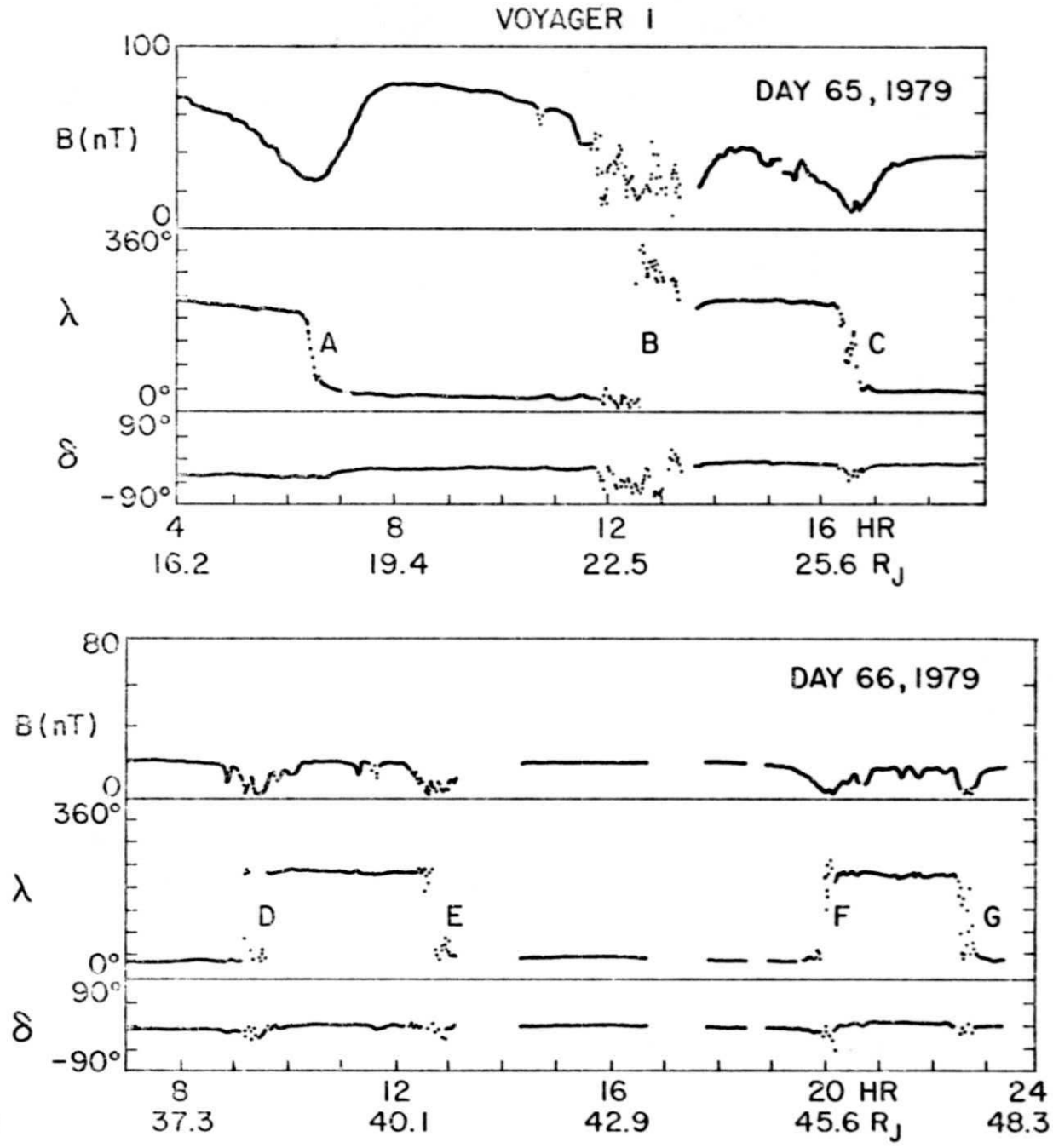
VOYAGER 1
DAY 65, 1979
B(nT)
100
0
360°
λ
0°
A
B
C
90°
δ
-90°
4
8
12
16 HR
16.2
19.4
22.5
25.6 R_J
DAY 66, 1979
B(nT)
80
0
360°
λ
0°
D
E
F
G
90°
δ
-90°
8
12
16
20 HR
24
37.3
40.1
42.9
45.6 R_J
48.3

FIGURE 4

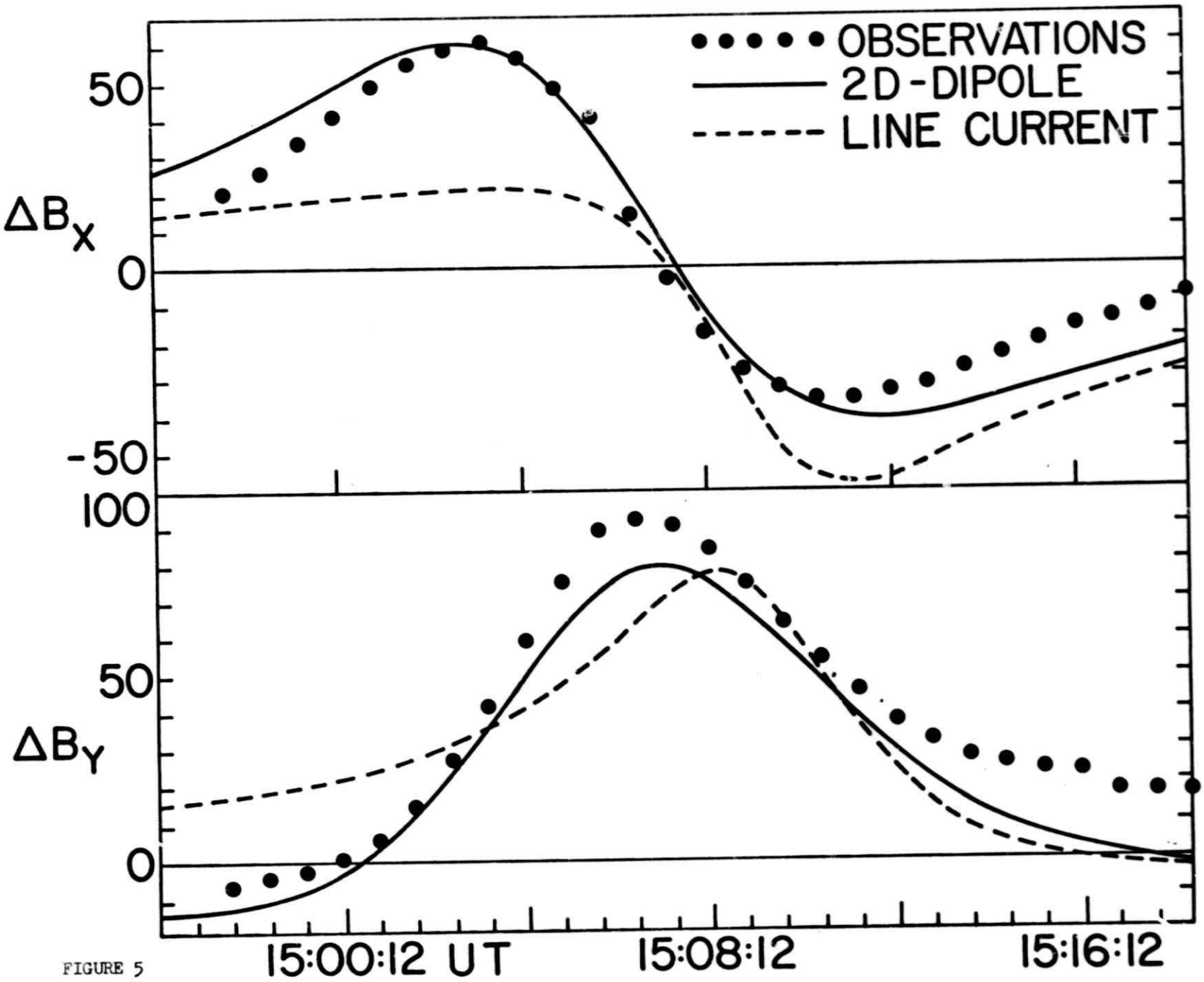
OBSERVATIONS
2D-DIPOLE
LINE CURRENT
50
0
-50
ΔBX
100
50
0
ΔBY
15:00:12 UT
15:08:12
15:16:12

FIGURE 5

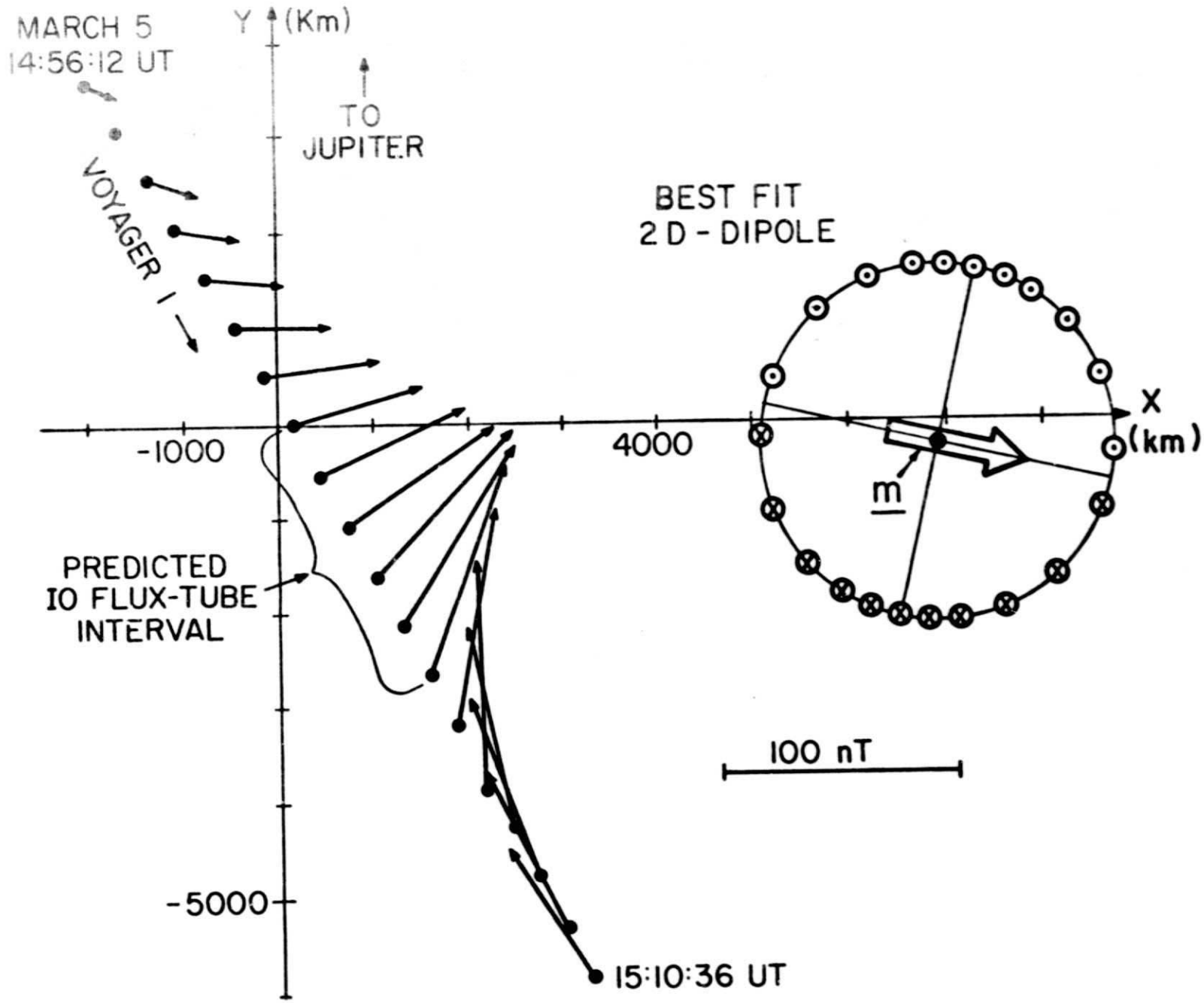
MARCH 5
14:56:12 UT
Y (Km)
TO
JUPITER
VOYAGER 1
BEST FIT
2 D - DIPOLE
X
(km)
-1000
4000
m
PREDICTED
IO FLUX-TUBE
INTERVAL
100 nT
-5000
15:10:36 UT

FIGURE 6

BIBLIOGRAPHIC DATA SHEET

1. Report No.	2. Government Accession No.	3. Recipient's Catalog No.
4. Title and Subtitle Magnetic Field Studies at Jupiter by Voyager 1: Preliminary Results		5. Report Date 6. Performing Organization Code
7. Author(s) N. F. Ness et al.		8. Performing Organization Report No.
9. Performing Organization Name and Address Laboratory for Extraterrestrial Physics GSFC		10. Work Unit No. 11. Contract or Grant No. 13. Type of Report and Period Covered
12. Sponsoring Agency Name and Address		14. Sponsoring Agency Code
15. Supplementary Notes		
16. Abstract Attached		
17. Key Words (Selected by Author(s))	18. Distribution Statement	

19. Security Classif. (of this report)	20. Security Classif. (of this page)	21. No. of Pages	22. Price*

*For sale by the National Technical Information Service, Springfield, Virginia 22151.

GSFC 25-44 (10/77)